minerals

MDPI

Article

Inhibitory Effects of Polysaccharides on the Dolomitization Reaction of Calcite at 200 °C

Yang Wei [1] and Hiromi Konishi [1,2,*]

[1] Department of Geology, Graduate School of Science and Technology, Niigata University, Niigata 950-2181, Japan; weiyangrm@163.com
[2] Department of Geology, Faculty of Science, Niigata University, Niigata 950-2181, Japan
* Correspondence: hkonishi@geo.sc.niigata-u.ac.jp

Abstract: This study investigates the impact of dissolved carboxymethyl cellulose (CMC) and agar on the dolomitization reaction of calcite at 200 °C. Previous studies have suggested that CMC and agar promote dolomite precipitation at room temperature. However, this study found that their decomposition products hinder the reaction at 200 °C, with uncertainty about their role at other temperatures. The inhibitory effect of the decomposition products could be attributed to their adsorption onto calcite surfaces, which hinders their dissolution. This results in a longer reaction induction period and replacement period. Regression analysis demonstrates that the 0.1 g/L agar and 0.2 g/L CMC series decrease the cation ordering rate of dolomite produced from synthetic calcite when compared with series without polysaccharides. In contrast, the 0.1 g/L CMC series shows a slight increase in the cation ordering rate compared with series without polysaccharides. The findings of this study suggest a notable potential impact of the decomposition products of polysaccharides on the ordering of dolomite, although it is uncertain whether they inhibit this ordering process. The inhibitory effect observed in the decomposition products of CMC and agar could also exist in the decomposition products of the extracellular polymeric substances (EPS) and bacteria cell walls found in sedimentary rocks during burial diagenesis. Therefore, further research is necessary to understand the role of EPS and bacteria cell walls in dolomitization, since their impact is not always predictable.

Keywords: dolomitization; cation ordering; dolomite problem; inhibition effect; carboxymethyl cellulose; agar; calcite

check for updates

Citation: Wei, Y.; Konishi, H. Inhibitory Effects of Polysaccharides on the Dolomitization Reaction of Calcite at 200 °C. *Minerals* **2024**, *14*, 721. https://doi.org/10.3390/min14070721

Academic Editor: Olev Vinn

Received: 25 May 2024
Revised: 6 July 2024
Accepted: 15 July 2024
Published: 18 July 2024

Copyright: © 2024 by the authors. Licensee MDPI, Basel, Switzerland. This article is an open access article distributed under the terms and conditions of the Creative Commons Attribution (CC BY) license (https://creativecommons.org/licenses/by/4.0/).

1. Introduction

Dolomite is a mineral composed of calcium magnesium carbonate, with the chemical formula $CaMg(CO_3)_2$. The crystal structure of dolomite consists of alternating layers of calcium and magnesium ions held together by carbonate ions. When the arrangement of Ca^{2+} and Mg^{2+} is completely disordered, dolomite takes on a calcite structure and is referred to as "disordered dolomite" or "very high magnesium calcite" (VHMC) [1]. The c-glide symmetry found in calcite is also present in this type of dolomite. Dolomite can be enriched in Ca^{2+} with the formula $Ca_{1+n}Mg_{1-n}(CO_3)_2$, also known as "calcian" [1–4]. Stoichiometric dolomite is distinguished by its nearly perfect 1:1 ratio of magnesium to calcium. However, naturally occurring sedimentary dolomite typically has a slightly higher percentage of calcium and is not perfectly ordered in terms of Ca^{2+} and Mg^{2+}, which is referred to as protodolomite [1]. In this paper, we categorize dolomite solely based on its proximity to the dolomite formula without considering the ordering state of dolomite when the prefixes "disordered" and "ordered" are not used.

The "dolomite problem" refers to the challenge of explaining the significant variability in dolomite production throughout geological time periods, as well as the difficulty of replicating dolomite formation under ambient lab conditions despite its presence in surface environments in the past [1,5–9]. There is no evidence to suggest that dolomite formed

during Earth's early history in the Hadean Eon. However, it did start appearing in carbonate formations during the subsequent Archean Eon, with dolomite being a predominant type of carbonate rock during this time [10]. Huge massive dolomite deposits were formed during the Neoproterozoic Era. During the Phanerozoic Eon, there were several significant periods of increased dolomite production in comparison with total carbonate rock, such as the Ordovician Period, Triassic Period, and Cretaceous Period [11]. It is suggested that there is a correlation between global dolomite contents and sea levels [12]. Conversely, dolomite formation is relatively uncommon in the Holocene epoch [12]. In current environments, dolomite is primarily found in hypersaline or alkaline lakes [13–24] and in cold seeps on ocean floors [25–34]. However, the amount of dolomite production in these environments is relatively small. Even though seawater is oversaturated with dolomite in modern times, its presence remains limited (PHREE QC Version 3 calculation).

Aragonite is more stable at higher pressures compared to calcite. In surface conditions, aragonite is metastable, while calcite and dolomite are stable [1,35]. Throughout Earth's history, there have been periods referred to as aragonite seas, where aragonite directly precipitates from seawater, and calcite seas where calcite precipitates from seawater [36–38]. These shifts are driven by fluctuations in the Mg/Ca ratio and concentration in seawater, which are influenced by changes in the movement of oceanic plates [38]. Morse et al.'s 1997 [39] experiments show that aragonite tends to precipitate with high Mg/Ca ratios, while calcite precipitates with low Mg/Ca ratios under surface conditions, supporting this hypothesis.

Observations of fibrous dolomite suggest the presence of dolomite seas, where dolomite precipitates directly from seawater [40–42]. It is speculated that dolomite could have formed under highly alkaline and anoxic sulfate-reducing conditions [40–42]. Zhang et al. (2012) [43] discovered that dissolved sulfide catalyzed dolomite precipitation at room temperature, further supporting the geological estimation. Additionally, there is a suggested connection with the extreme Neoproterozoic glacial events [40].

One possible reason for the difficulty in incorporating Mg^{2+} into the dolomite structure is the formation of strong Mg^{2+}–water complexes in aqueous solutions, which creates a significant barrier to dehydration [5,44–46]. This explanation does not align with the fact that Mg-containing carbonates with the same structure as dolomite, such as norsethite $BaMg(CO_3)_2$ and $PbMg(CO_3)_2$, easily precipitate in water [47–49]. However, this explanation does help to clarify the catalytic effect of polysaccharides. The presence of polysaccharides such as CMC and agar loosens the bonding between the Mg hydration shells, allowing Mg^{2+} to enter the dolomite structure [50,51]. This occurrence can be attributed to the ability of carboxyl groups present in the polysaccharides to form complexes with Mg^{2+}, resulting in the competitive attraction of Mg^{2+} over water molecules [50–53].

Certain microbes, such as sulfate-reducing bacteria (SRB), halophilic bacteria, green sulfur bacteria, cyanobacteria, and archaea, play a role in the formation of dolomite through a process known as microbial mediation [8,9,16,54–67]. The exact mechanism by which bacteria facilitate dolomite formation is not fully understood. Almost all microbes produce carbonic anhydrase enzymes as part of their metabolic functions. These enzymes are crucial for converting carbon dioxide (CO_2) into bicarbonate ions, which are essential for various physiological processes such as cellular respiration and pH regulation. Some bacteria utilize carbonic anhydrase enzymes to capture and convert CO_2 into bicarbonate ions, which then combine with other ions to create calcium carbonate [68]. CO_2 emitted through respiration itself may serve as a carbon source, in addition to CO_2 from the surrounding environment. This process may contribute to dolomite mineralization to some extent. Additionally, bacteria have cell walls primarily composed of polysaccharides and lipids, and produce EPS, which are primarily composed of exopolysaccharides. These polysaccharides may function as a catalyst to facilitate the formation of dolomite [52,69–71].

In a study conducted by Kim et al. in 2023 [72] using atomistic simulations, it was demonstrated that dolomite initially precipitates a cation-disordered surface, with high surface strains inhibiting further crystal growth. However, mild undersaturation tends to

dissolve these disordered regions preferentially, enabling increased order upon reprecipitation. Additionally, Kim et al. in 2023 [72] claimed that ordered dolomite was observed through in-situ TEM experiments.

Disordered dolomite has been observed to precipitate in experiments involving bacteria cultures [1], polysaccharide-containing solutions [50,52], and low-temperature inorganic synthesis conducted at room temperature [73]. However, Kim et al. in 2023 [72] managed to inorganically produce ordered dolomite at room temperature. It is uncertain whether this mechanism fully explains dolomite formation in nature, as naturally occurring sedimentary dolomite is typically protodolomite and does not exhibit perfect ordering. However, there is a belief that the ordering of cations in dolomite could be improved through multiple dissolution and precipitation cycles. This involves altering the saturation and undersaturation of the solution repeatedly, potentially impacting the structure of the dolomite crystals.

This study aimed to investigate the catalytic potential of EPS and bacterial cell walls in dolomitization, as well as other natural polysaccharides, by testing the catalytic activity of two specific polysaccharides—CMC and agar—which can be considered analogs of EPS and bacterial cell walls. The objective was to gain insights into the role of natural polysaccharides in the geological process of dolomitization.

2. Materials and Methods

2.1. High-Temperature Dolomite Synthesis Experiments

Experiments were conducted in Teflon-lined stainless-steel batch reactors at 200 °C, where solid reactant calcium carbonate phases were reacted with experimental solutions. The chosen temperature of 200 °C allowed for relatively short reaction times to generate dolomite at favorable time scales for lab experimental work, to test the impact of polysaccharide. Additionally, the temperature was chosen because deep burial diagenesis reaches a maximum temperature of 200 °C.

The experiment utilized reagent-grade synthetic calcite powder (Product Number 030-00385, FUJIFILM Wako Pure Chemical Corporation, Osaka, Japan), and cleaved thin calcite crystals (about 0.5 mm) obtained by knocking down geological calcite single crystals 1–2 cm in size (Tokyo-Science Co., Ltd., Tokyo, Japan) as the initial solid reactant calcium carbonate phase. Mg^{2+} and Ca^{2+} were supplied by Mg-Ca-Cl solution (Mg:Ca = 1:1 for molar concentration) produced by dissolving magnesium chloride hexahydrate and calcium chloride dihydrate in distilled water.

For each experiment, 0.25 g of solid reactant calcium carbonate phase was added to a 36 mL experimental solution composed of Mg-Ca-Cl solution with or without the addition of polysaccharide solutions. CMC and agar were tested as analogs for dissolved carbohydrates found in sediment pore fluids, which are produced by the degradation of organic matter in sediments. Additionally, they were tested as analogs for EPS and bacterial cell walls, which are also composed of polysaccharides. After adjusting the pH to 8.5, the solid reactant and experimental solution mixture was loaded into a reactor, sealed, and heated at 200 °C for a chosen duration in a convection oven. To investigate the effects of adding CMC or agar, parallel control experiments were conducted in experimental solutions composed of 36 mL of 0.5 M Mg-Ca-Cl solution without CMC and agar. After cooling to room temperature, the final pH of the reaction solution was measured before decanting and discarding the fluid.

The solid product was transferred to a centrifuge tube and rinsed in distilled water, with the liquid being decanted after centrifugation at 4000 rotations per minute for 10 min. The product obtained from the cleaved thin calcite crystal series was also transferred to a centrifuge tube and meticulously cleaned in distilled water without being centrifuged. After repeating the cleaning procedure three times, the collected solid product was dried at 40 °C for X-ray diffraction (XRD) and scanning electron microscopy (SEM) investigations.

To prepare the experimental solutions, we combined 30 mL of 0.6 M Mg-Ca-Cl solution with one of three 6 mL stock solutions of CMC, which had concentrations of 0.6 g/L, 1.2 g/L, and 1.8 g/L. Similarly, we prepared experimental solutions containing agar concentrations of

0.1 g/L, 0.2 g/L, and 0.3 g/L by mixing 30 mL of 0.6 M Mg-Ca-Cl solution with one of three 6 mL stock solutions of agar, which had concentrations of 0.6 g/L, 1.2 g/L, and 1.8 g/L.

To prepare each CMC stock solution with concentrations of 0.6 g/L, 1.2 g/L, and 1.8 g/L, we dissolved 60 mg, 120 mg, and 180 mg of the sodium salt of CMC (Product Number 05-1760, Sigma-Aldrich Japan G.K., Tokyo, Japan) in 100 mL of distilled water. Similarly, we prepared agar stock solutions with concentrations of 0.1 g/L, 0.2 g/L, and 0.3 g/L by dissolving 60 mg, 120 mg, and 180 mg of agar powder (Product Number 010-15815, FUJIFILM Wako Pure Chemical Corporation, Osaka, Japan) in 100 mL of distilled water, respectively. We kept the agar stock solutions at 45 °C to prevent gelation.

Furthermore, experiments involving the heated CMC were conducted. During these trials, a solution containing 0.1 g/L of CMC was initially heated at 200 °C for 48 h. Subsequently, 6 mL of this heated solution was mixed with 30 mL of a 0.6 M Mg-Ca-Cl solution to create the experimental solution.

2.2. XRD and SEM Analyses

To prepare the powdered samples of the synthetic calcite series for XRD analysis, the samples were hand-pulverized using an agate mortar and pestle. The prepared samples were mounted on a low-background silicon plate, and diffraction data were collected over a range of 3 to 70° 2θ with a scan speed of 2° 2θ per minute. The XRD analysis was conducted using a Rigaku Ultima-IV diffractometer (Tokyo, Japan) operating at 40 kV and 40 mA with Cu-Kα radiation, a 2/3 degree divergence slit, and a 0.6 mm receiving slit.

The reaction progress was measured as the peak–height ratio of the dolomite (104) peak divided by the dolomite (104) peak plus the initial calcium carbonate phase (104) peak, and reported as the percent product [74]. The stoichiometry of dolomite was determined using the following equation: mol% $CaCO_3$ = 333.33 × d(104) − 911.99 [75]. The degree of cation ordering in the dolomite lattice was determined by the proportions of the intensities of (015) peak and (110) peak [1,4,76].

To observe the samples of reaction products from the cleaved thin calcite crystal series, SEM observations were conducted using the JEOL JSM-IT100 Scanning Electron Microscope (Tokyo, Japan) after ~20 nm of carbon coating.

2.3. Transmission Electron Microscopy (TEM)

The synthetic products were crushed between two glass slides with a drop of distilled water, and the resulting suspension was deposited onto a lacey carbon film supported by a Cu TEM grid and air-dried for TEM observations. High-resolution transmission electron microscopy (HRTEM) analysis was performed using a JEOL JEM-2010 microscope (Tokyo, Japan) with an accelerating voltage of 200 kV. The resulting images were captured on imaging plates.

3. Results and Discussion

3.1. Reaction Pathway

The XRD analysis of the reaction products identified three stages of dolomitization reaction. The first stage, known as the induction stage, concludes with the initial detection of calcian dolomite by XRD. The second stage is characterized by rapid replacement, where calcite reactants are swiftly substituted with calcian dolomite. This stage begins with a gradual start and exhibits a sharp increase towards the end, resulting in approximately 90% replacement of calcite reactants based on our definition. The third stage entails the recrystallization process from calcian dolomite to ideal dolomite. Although not a perfect match, we consistently observed these three stages of the dolomitization reaction through XRD analysis of the reaction products obtained from experiments conducted both with and without polysaccharides (Figure 1).

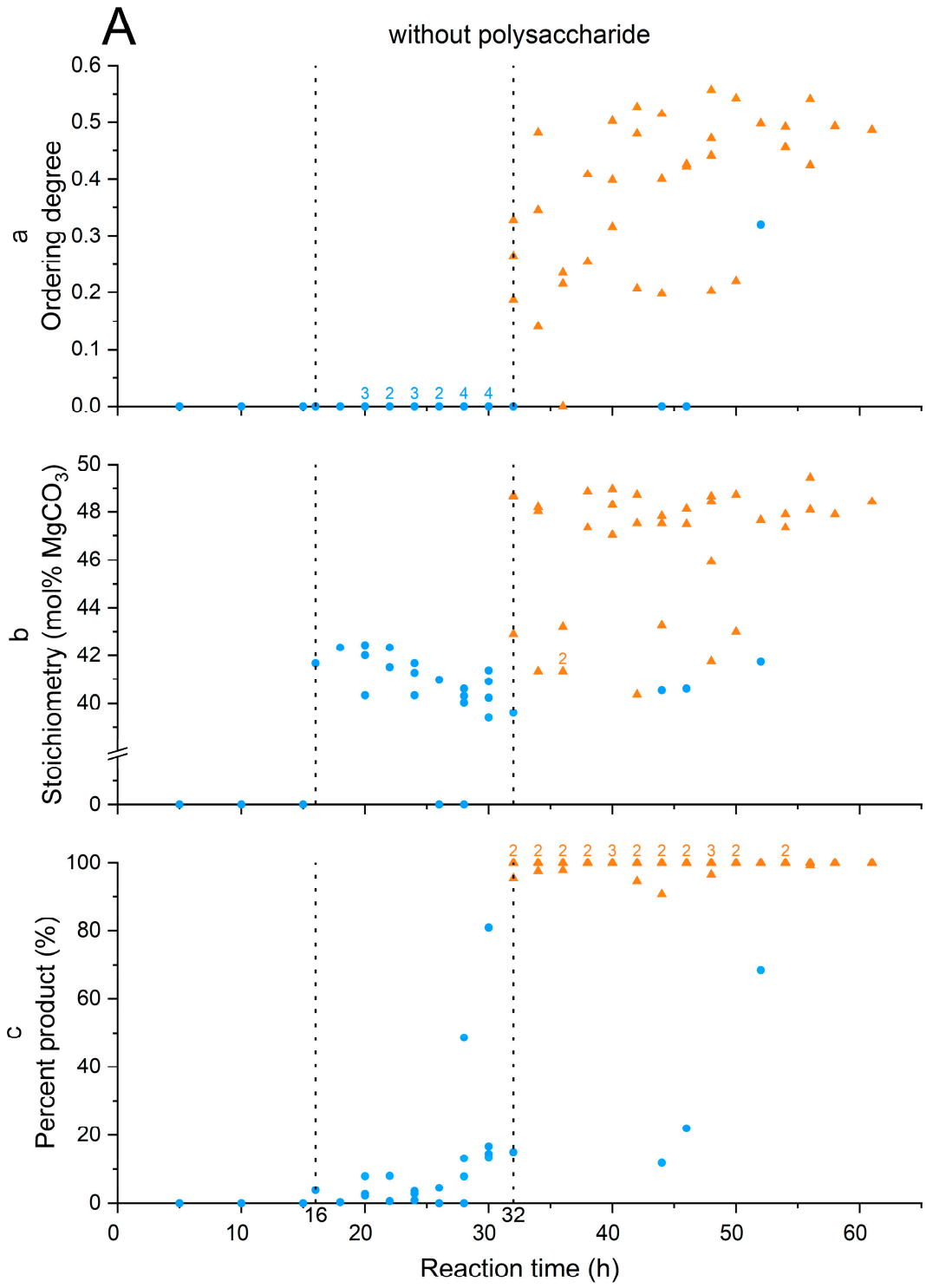


Figure 1. *Cont.*

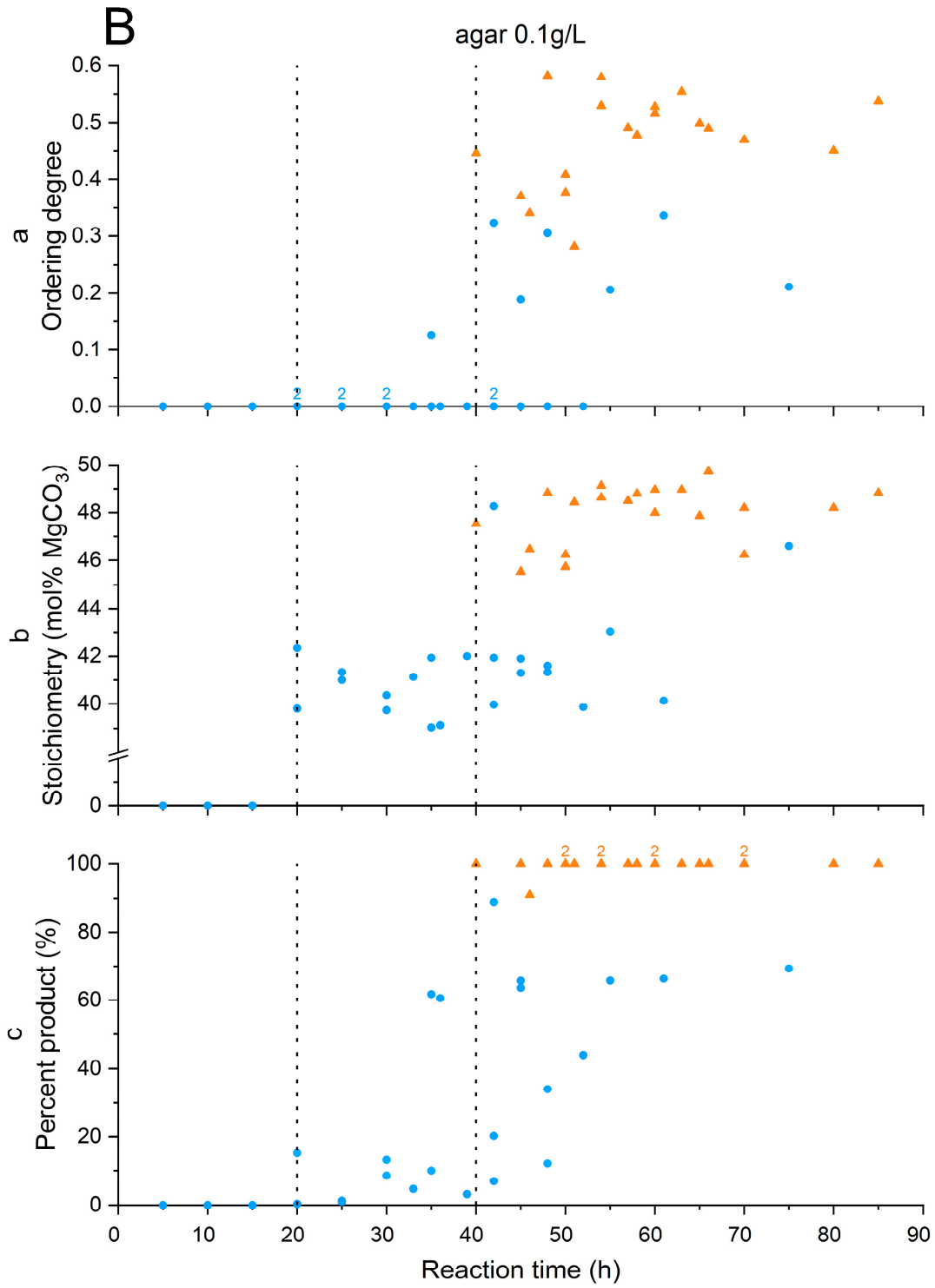


Figure 1. *Cont.*

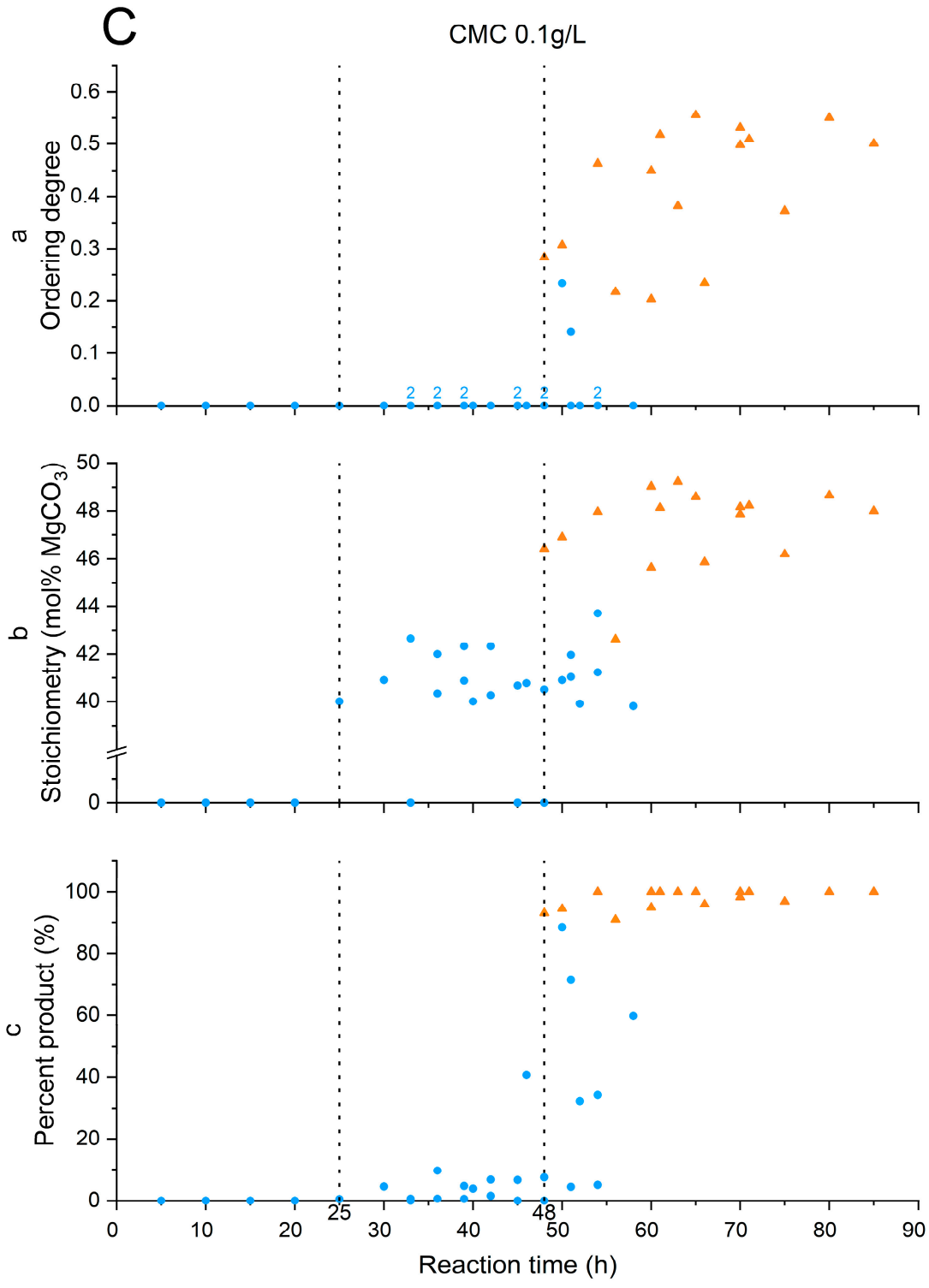


Figure 1. *Cont.*

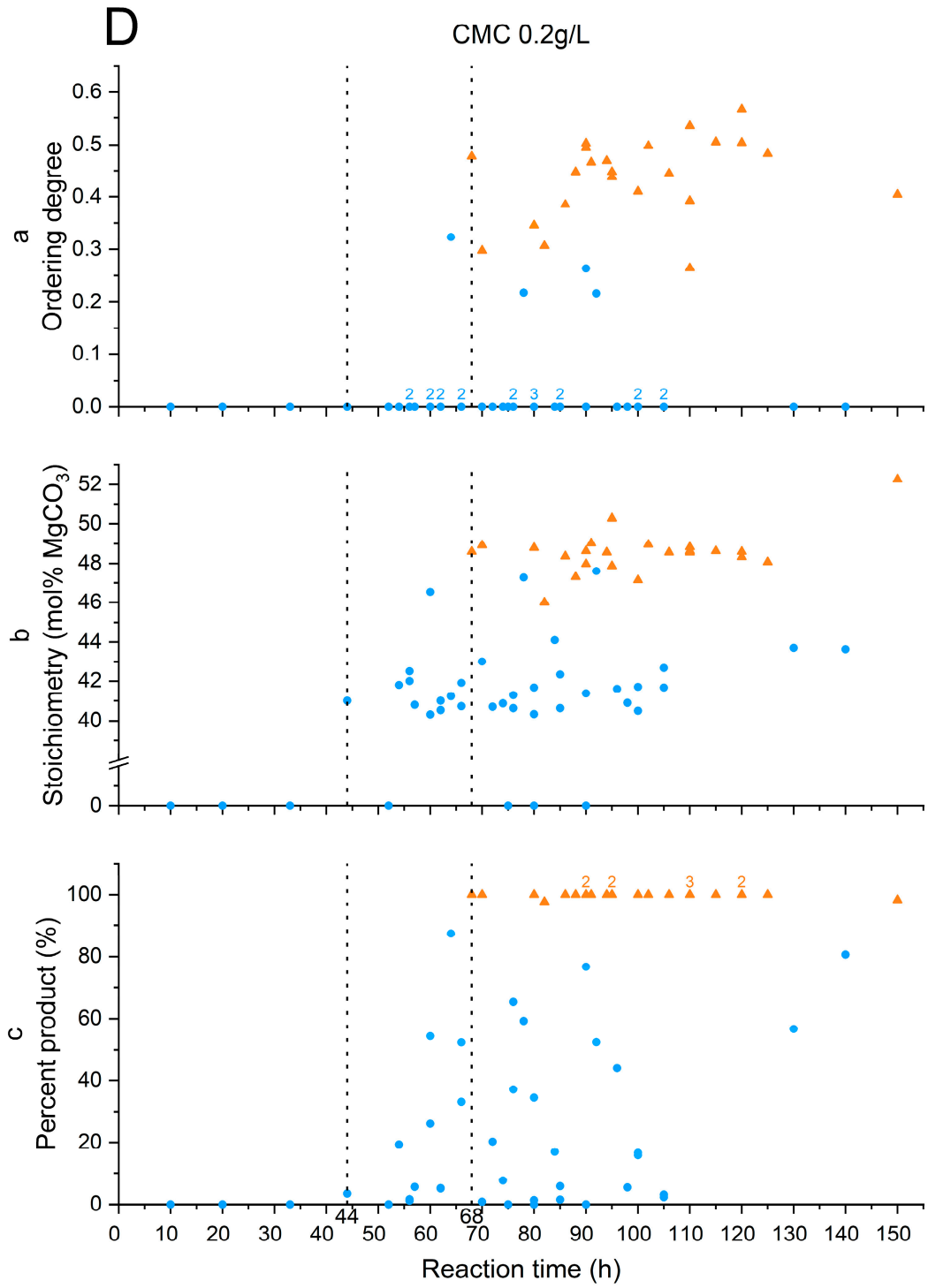


Figure 1. The graphs show the progress of the dolomitization reaction of synthetic calcite in various experiments: (**A**) parallel control experiment (referred to as "without polysaccharide"), (**B**) agar 0.1 g/L series experiment, (**C**) CMC 0.1 g/L series experiment, and (**D**) CMC 0.2 g/L series experiment. Dashed vertical lines mark the boundaries of the three reaction stages, with numbers indicating the total overlapping points at each position. Each graph has three cross-plots: (**a**) ordering degree vs. reaction time (h), (**b**) stoichiometry (mol% $MgCO_3$) vs. reaction time (h), and (**c**) percentage of product vs. reaction time (h). In the figures, blue circles denote dolomite abundances below 90%, while orange triangles indicate abundances exceeding 90%. The data points represent multiple experiment batches, so the boundaries of the three stages were established at the point where the characteristics specific to each stage initially appeared. The numbers above or below the points indicate the total number of overlapping points at each position.

3.2. Evolution of pH

In the parallel control experiments, it is consistently observed that the final pH after the reaction is generally higher than the initial pH. However, in the polysaccharide series of experiments, there is a notable occurrence of final pH values that are lower than the initial pH. This is particularly evident in the experiments conducted prior to reaching the end of the replacement stage (refer to Table S1 in Supplementary Materials for specific data).

3.3. Stoichiometry and Cation Ordering

The initial products of Mg-Ca carbonate are classified as calcian dolomite that are always relatively enriched in calcium compared with stoichiometric dolomite. During the rapid replacement stage, calcian dolomite typically has a $MgCO_3$ content of 39.03–42.67 mol%, with one exception that was heated for 60 h, achieving 46.53 mol% $MgCO_3$ in the 0.2 g/L CMC series. Generally, calcian dolomite lacks ordering, except for two cases: (1) a sample heated for 35 h in the 0.1 g/L agar series with an ordering index of 0.13, and (2) a sample heated for 64 h in the 0.2 g/L CMC series with an ordering index of 0.32.

During the recrystallization stage, the stoichiometry of dolomite significantly increases towards 50 mol% $MgCO_3$, with one notable exception: a sample heated for 150 h, achieving 98.3% conversion but a $MgCO_3$ content of 52.27 mol% in a 0.2 g/L CMC series. After 100% replacement, the majority of the final products have $MgCO_3$ contents ranging from 47.03 to 50.27 mol%, with a few exceptions displaying $MgCO_3$ contents ranging from 41.33 to 46.23 mol% (Figure 1).

Similar to previous research conducted under high temperature [77–79], the initial calcian dolomite products are always free from detectable cation ordering, as observed through XRD analysis. The (015) ordering peak is typically detectable after 90% replacement of the initial reactant. In agar 0.1 g/L series experiments, the (015) ordering peak can even be detected when only 34% of the initial reactant has been replaced. As the reaction proceeds, the ordering degree increases to a maximum. In general, longer heating times result in a higher degree of ordering, with a stoichiometry of 49.9 mol% $MgCO_3$ and an ordering degree of 0.62 achieved after 228 h of heating (see Table S1).

It is widely accepted that as time progresses, more replacement product, higher stoichiometry of dolomite, and a greater ordering degree are typically achieved. However, as depicted in Figure 1, similar to the findings of prior studies [79], there is a significant amount of variation in the reaction time according to the percentage of product, stoichiometry, and ordering degree. This variability is particularly noticeable in the experiments involving the synthetic calcite series. One possible explanation for this scatter could be the localized small-scale heterogeneity in the surrounding solution due to certain reactants being encapsulated within the products [79].

3.4. Polysaccharides' Impact on Calcite Dolomitization

We found that all series containing polysaccharides always took longer to react (Figure 2 and Table 1). Adding dissolved polysaccharides to the initial experimental solutions prolongs the induction period of the dolomitization reaction (Figure 1 and Table 1). In particular, in the CMC 0.1 g/L and CMC 0.2 g/L series experiments, the induction periods were significantly extended. The slight delay in the induction period for the agar 0.1 g/L series compared to the parallel control group could be attributed to agar's weaker inhibitory effects and lower concentration. Additionally, this study assessed the impact of solutions with higher concentrations of organic substances and found significant inhibition with 0.2 g/L agar and 0.3 g/L CMC. Notably, there was no formation of calcian dolomite even after 200 and 80 h of heating, respectively (see Table S1).

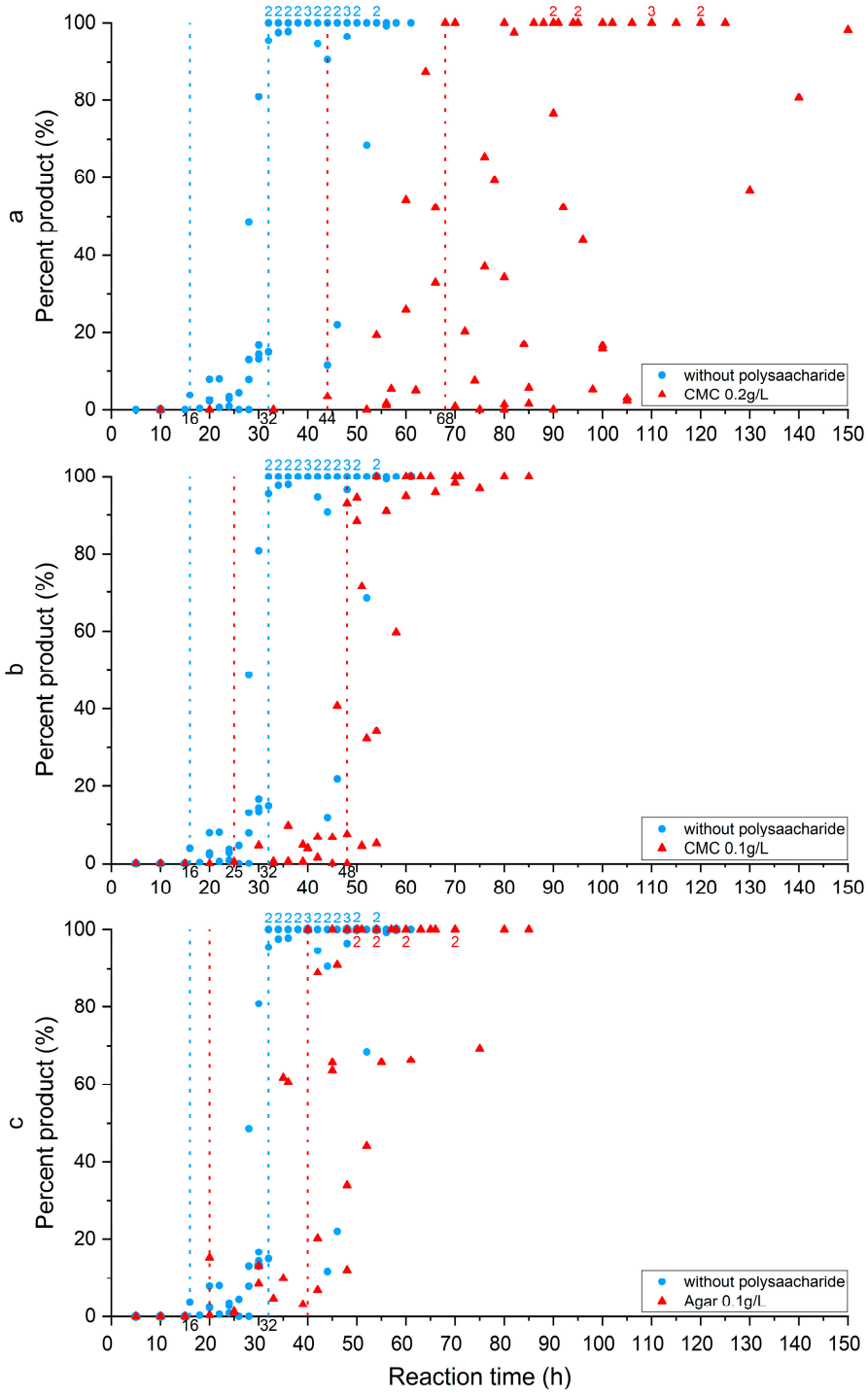


Figure 2. Percentage of dolomite product plotted against reaction time. Data points from experiments in the without-polysaccharide series are plotted in blue, while data points from experiments in the with-polysaccharide series are plotted in red. Colored dashed vertical lines demarcate the boundaries of the three reaction stages in the respective experiments. In all three plots (**a**–**c**), the blue data points are shifted to the left on the reaction time axis compared to the red data points. This indicates that the dolomitization reaction was delayed in the experiments with polysaccharides compared with the parallel control experiments in the without-polysaccharide series. The numbers above or below the points indicate the total number of overlapping points at each position.

Table 1. Reaction stage times for dolomitization reaction as shown in Figure 1.

Additive	Time of Induction Stage End (h)	Time of Replacement Stage End (h)
without polysaccharide	16	32
agar 0.1 g/L	20	40
CMC 0.1 g/L	25	48
CMC 0.2 g/L	44	68

When compared to the parallel control experiments, all polysaccharide series experiments exhibited longer replacement stage lengths. In the replacement stage, CMC had a more significant effect than agar. The addition of 0.2 g/L CMC had the most notable impact, prolonging the stage length to 1.5 times that of the parallel control experiments.

Besides the longer induction period, the impact of polysaccharides on the rate of cation ordering should also be considered. Figure 3 displays the ordering index plotted against reaction time (h). Logarithmic fitting curves from various experimental series reveal that (1) the addition of 0.1 g/L agar and 0.2 g/L CMC decelerates the cation ordering rate of dolomite formed from synthetic calcite when compared with series lacking polysaccharides. (2) The series with 0.2 g/L CMC exhibits a significantly reduced cation ordering rate compared with the series without polysaccharides. (3) Conversely, the presence of 0.1 g/L CMC slightly boosts the cation ordering rate of dolomite produced from synthetic calcite in comparison with series without polysaccharides.

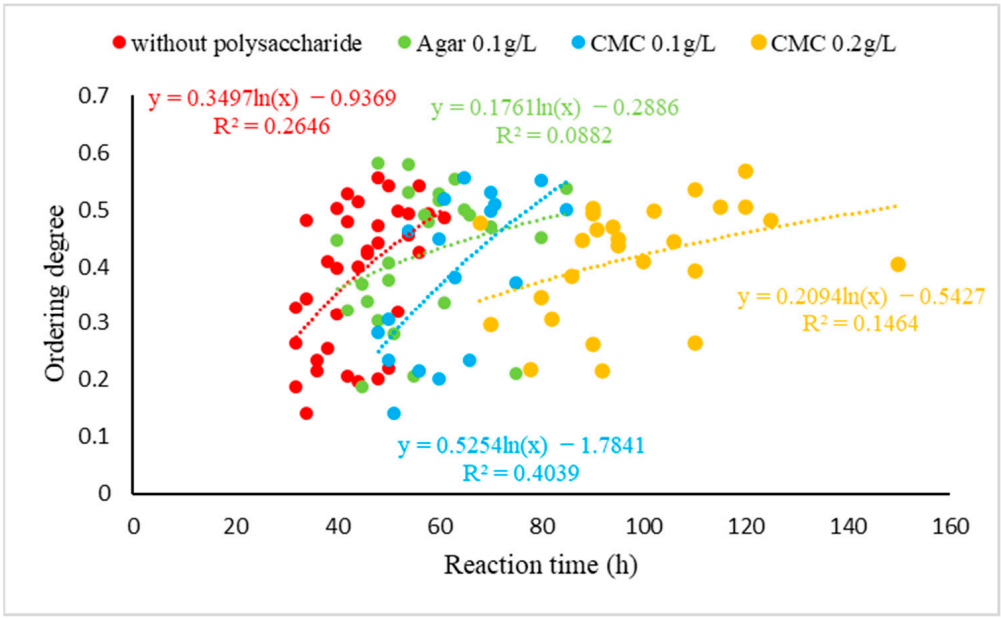


Figure 3. Cross-plot of the ordering degree against reaction time (h) for the synthetic calcite series.

The slope of the logarithmic curve in a cross-plot of ordering degree against reaction time (h) varies depending on the concentration of polysaccharides, suggesting a significant potential influence of polysaccharides on the ordering of dolomite. The ordering process of dolomite in hydrothermal conditions involves a dissolution and precipitation process rather than the diffusion of cations in solid dolomite crystal. Therefore, it is reasonable to assume that polysaccharides affect the ordering of dolomite, but further investigation is needed due to the low R^2 value of most fitting curves. Consequently, we cannot conclude that polysaccharides inhibit the cation ordering of dolomite at this point.

3.5. SEM Studies of Cleaved Calcite Crystal Reaction Products

The decomposition of dissolved CMC of high concentration at 200 °C caused the entire reaction solution to turn dark brown, with the collected reaction products also turning brown. This indicates that specific decomposition substances were adsorbed onto the surface of the calcite.

SEM studies have revealed that in controlled experiments without polysaccharides using cleaved thin calcites, the calcite (104) surface only exhibits etch pits (Figure 4). However, when experiments were conducted using the 0.1 g/L CMC series and 0.2 g/L agar series, the surface morphology changed to include micropyramids. Various morphological features were observed on the calcite (104) surface, including microneedles, pyramidal hillocks, microcone-like protrusions, parallel platy microstructures, typical quadrangle micropyramids, irregular micropyramids with tips, typical hexagon micropyramids, and densely packed hillocks, as identified in previous literature descriptions of micropyramids [80–83]. These changes indicate preferential dissolution during the reaction (Figure 5), suggesting that decomposition substances could impact the dolomitization reaction.

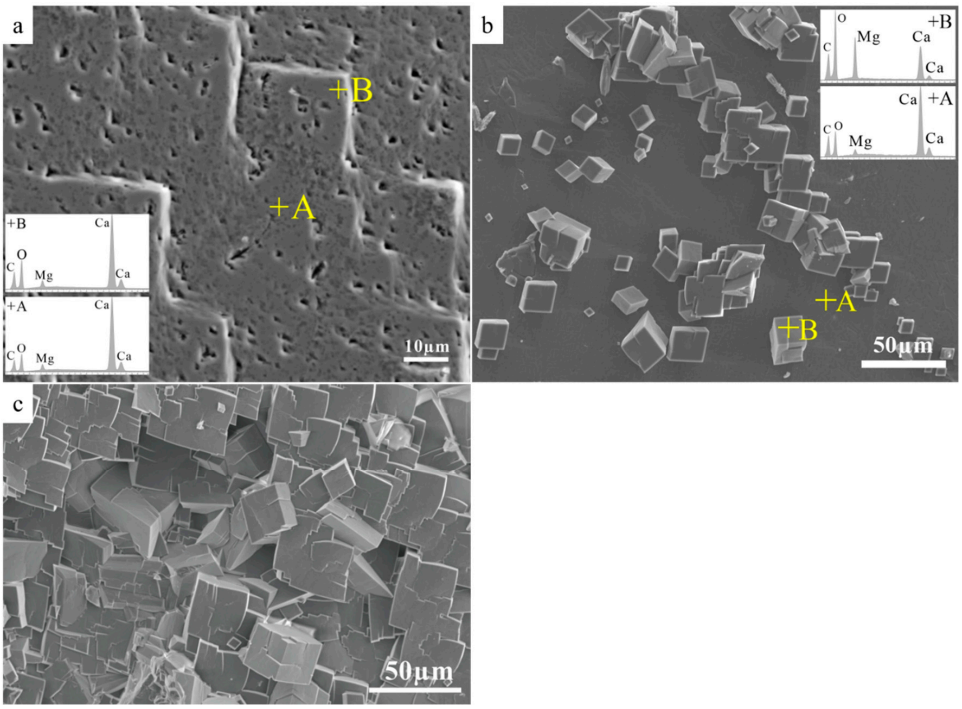


Figure 4. SEM images of reaction products from control experiments without polysaccharides using cleaved calcite. Etch pits on the calcite (104) plane are shown after 120 h (**a**). Rhombohedral dolomite crystallites at 150 h (**b**) form on the calcite (104) plane and continue to grow, covering the surface after 250 h (**c**). EDS spectra were inserted in images (**a**,**b**), with the analyzing points denoted by yellow pluses (+).

3.6. Calcite Dissolution Inhibition by Surface Site Inhibition

In the with-polysaccharide series experiments, it was found that a significant number of final pH values did not exceed 7, particularly in samples collected before the replacement stage was completed. This slightly acidic environment was not conducive to dolomite formation. However, when experiments were conducted using CMC solutions heated at 200 °C for 48 h, the final pH values increased in all cases. Nevertheless, even after 320 h of heating, no newly detectable dolomite was observed, ruling out the possibility that the pH decrease inhibits dolomitization, and indicating that polysaccharide decomposition products impede dolomitization (Table 2).

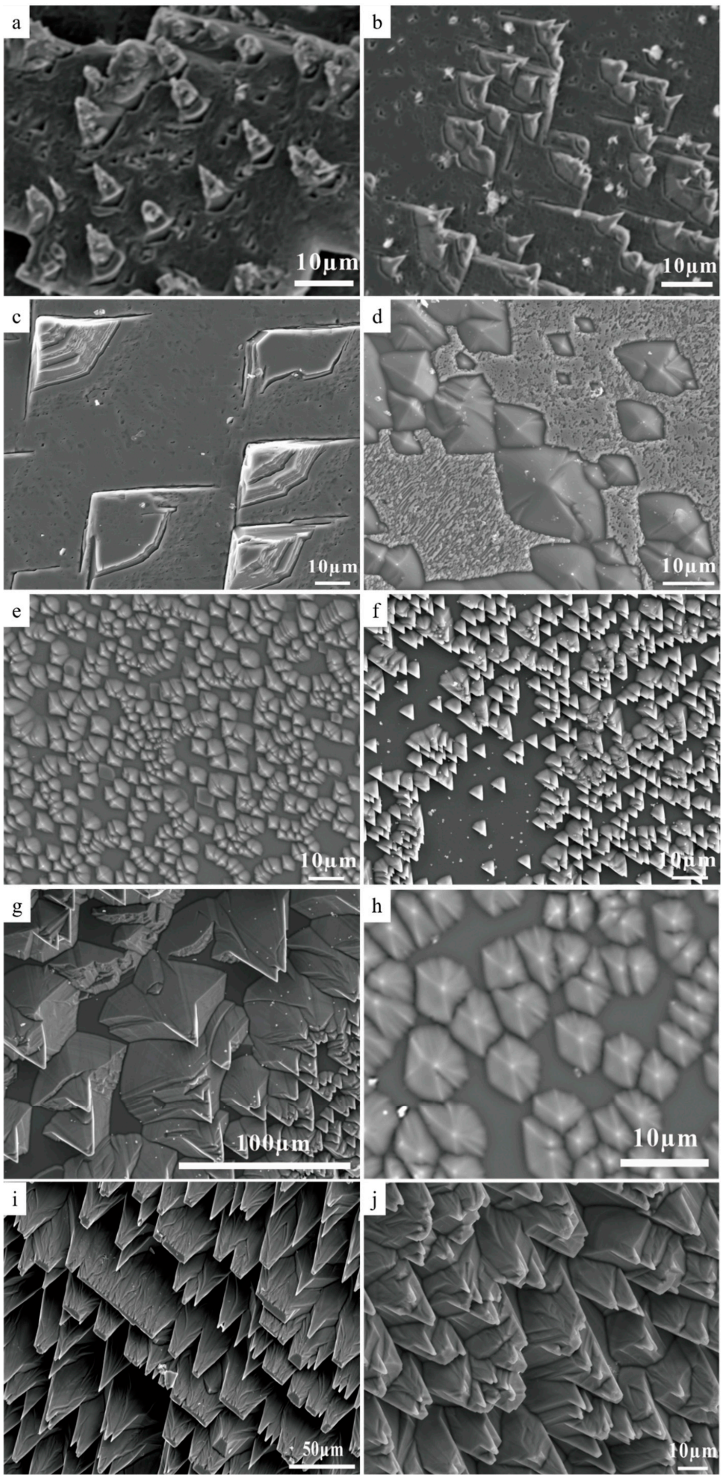


Figure 5. SEM images of reaction products from the 0.1 g/L CMC series (**a**–**d**) and 0.2 g/L agar series (**e**–**j**) are presented, with each series separately heated for varying durations. In the CMC series, microneedles were observed on the calcite (104) plane after 120 h (**a**,**b**), followed by pyramidal hillocks after 150 h (**c**) and the formation of quadrangle typical micropyramids after 250 h (**d**). The agar series exhibited tiny typical quadrangle micropyramids, microcone-like protrusions, and large-sized irregular micropyramids with tips after 130 h ((**e**–**g**), respectively), and hexagon typical micropyramids after 200 h (**h**), followed by parallel platy microstructures after 250 h (**i**), and densely packed hillocks after 350 h (**j**). The names of the microstructures are based on previous literature [80–83].

Table 2. pH values of experiments using 0.1 g/L CMC solution heated at 200 °C for 48 h. The error is ±0.11 pH.

	Initial pH	Final pH	Heating Time (h)
No.1	8.48	9.26	80
No.2	8.50	8.68	100
No.3	8.50	9.20	120
No.4	8.48	8.78	320

The inhibition of calcite growth and dissolution via the surface site inhibition induced by additives has been widely studied and applied [84–89]. This phenomenon involves the adsorption of additives on the active sites of calcite surfaces, preventing them from dissolving and thus making the remaining sites preferentially dissolve. As shown in Figure 5, this results in adsorbed sites becoming micropyramids, microcone-like protrusions, or hillocks. It has also been suggested that the more additives attach to the crystal surface, the lower the dissolution rate of calcite [80].

The inhibition effect observed is primarily attributed to the decomposition products of polysaccharides rather than the dissolved CMC and agar themselves. Cellulose, a type of polysaccharide, was observed to decompose at 200 °C, resulting in a water-soluble fraction, an acetone-soluble fraction, and a solid residue [90]. The inhibition effect may be linked to the degradation of polysaccharides at high temperatures. It is expected that the same additive at a constant concentration typically exhibits only one adsorption mode, resulting in a singular morphological structure. The numerous morphological structures observed via SEM on calcite surfaces indicate responses to the adsorption behavior of different substance species. This does not rule out the possibility that changes in the concentration of single-substance species throughout the reaction may generate multiple morphological structures.

3.7. HRTEM Observation of Antiphase Boundaries (APBs) in Dolomite

APBs were identified in dolomite originating from calcite (Figure 6). Typically, APBs form where ordering commences at various points within a disordered crystal. If ordering (OX) initiates at two distinct locations in a disordered state, some regions align without discrepancies, resulting in a sequence like . . .OXOX. . ., while others exhibit mismatches such as . . .OXXOX. . . Although clear instances have not been reported to the best of our knowledge, similar phenomena could arise in epitaxial growth. Ordering progression through the repetitive dissolution and precipitation of calcian dolomite, coupled with epitaxial growth at multiple locations, could potentially lead to the development of APBs. The observed APBs likely formed during epitaxial growth when dissolution and precipitation repeated during the recrystallization stage. Upon observing the SEM image of dolomite on cleaved calcite, it is apparent that dolomite overlies the calcite rather than having the Mg^{2+} in the surrounding Mg-Ca-Cl solution replace the Ca^{2+} in calcite (Figure 4b,c). The presence of observed APBs in dolomite may be attributed to epitaxial growth rather than cation diffusion within solid dolomite.

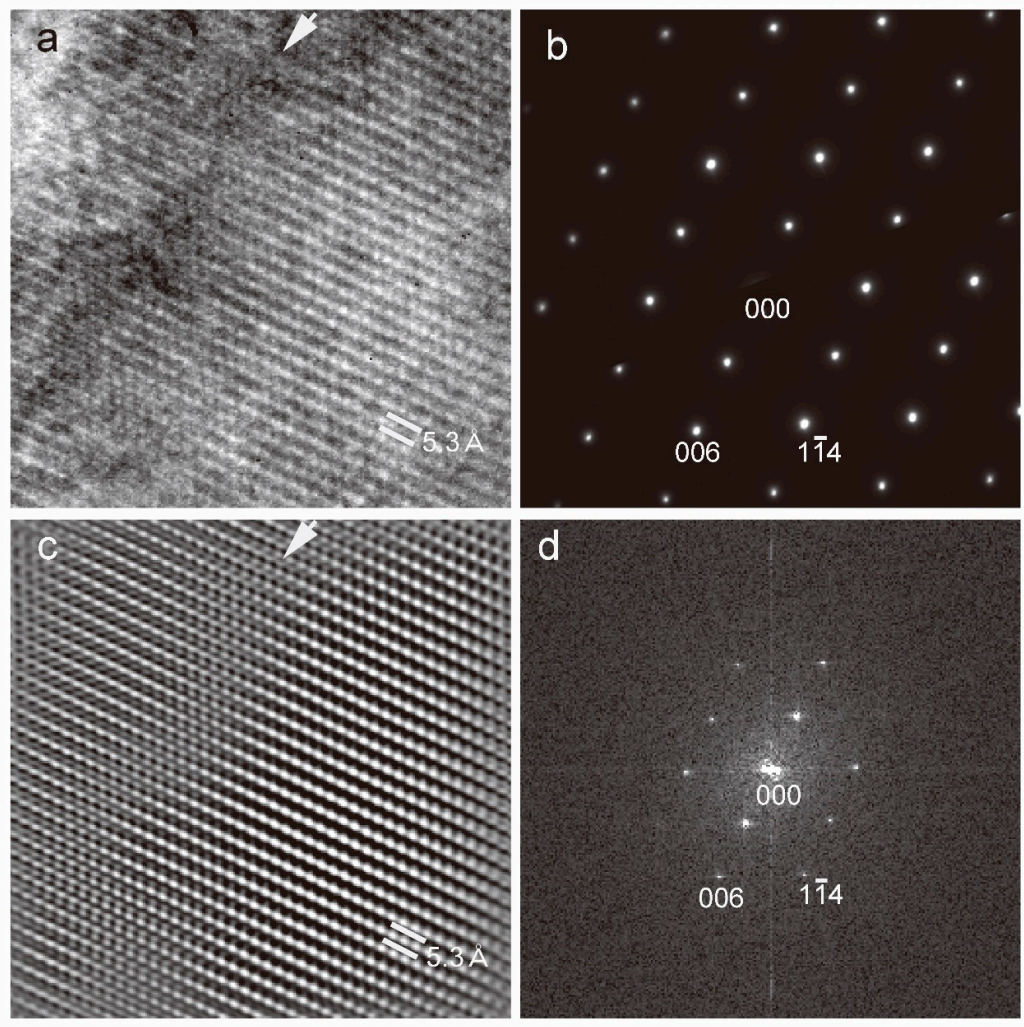


Figure 6. The [110] HRTEM image of an APB in dolomite is shown after being heated for 61 h at 200 °C (**a**), along with the corresponding electron diffraction (ED) pattern (**b**). The Fast Fourier Transform (FFT)-filtered image (**a**) of (**c**) and its FFT (**d**) are also presented. Arrows in images (**a**,**c**) point to the location of the APB.

4. Implications

This study found that at 200 °C, which is considered the upper temperature limit [91], CMC and agar inhibit the dolomitization of calcite, in contrast to their ability to promote dolomite precipitation at room temperature. However, the specific temperature at which this inhibitory effect occurs is still unknown. Since CMC and agar are polysaccharides similar to EPS and bacterial cell walls, it is possible that the inhibitory effect is linked to the decomposition products of these substances. Along with bacteria and other microorganisms, terrestrial plants, as well as various marine organisms such as phytoplankton, zooplankton, macroalgae, seaweeds, algal blooms, and marine snow, contribute polysaccharides to marine environments, which eventually end up in sedimentary deposits. As these polysaccharides persist in sedimentary rocks, their inhibitory effect may become evident during burial diagenesis.

If the inhibitory effect occurs at lower or moderate temperatures (below 200 °C), it could have a significant impact on the dolomitization process in burial diagenesis. This inhibition could lengthen the dolomitization reaction and lead to slower or potentially reduced dolomitization. In sedimentary rocks where decomposed polysaccharides remain, and in resedimented deposits that contain such decomposed polysaccharides, dolomitization may be impeded even at room temperature.

This study did not offer definitive evidence that the decomposition products of CMC and agar can directly impact the cation ordering process of dolomite and potentially delay cation ordering. Should the decomposition products of polysaccharides attach to surface sites in calcian dolomite similar to calcite, they might indeed slow down the cation ordering process. This is because the cation ordering process of dolomite could entail both dissolution and precipitation, rather than solely cation diffusion within solid dolomite.

Studies have shown that specific organic materials can enhance the dissolution of dolomite [92]. Sedimentary rocks commonly harbor a range of organic materials such as EPS, bacterial cell walls, their decomposition by-products, and diagenetic organic substances. Additional research is needed to ascertain the impact of each organic component on dolomitization processes and their role in the development of dolomite formations.

Supplementary Materials: The following supporting information can be downloaded at https://www.mdpi.com/article/10.3390/min14070721/s1: Table S1: Raw datasets of the hydrothermal experiments using synthetic calcite.

Author Contributions: H.K., as the principal investigator, led the conception of the research project and collaborated with Y.W. in developing the experimental design. H.K. performed the TEM measurements, while Y.W. conducted the hydrothermal experiments, XRD, and SEM measurements. Y.W. wrote the manuscript with contributions from H.K. All authors have read and agreed to the published version of the manuscript.

Funding: H.K. acknowledges support from JSPS KAKENHI Grant Number JP26400512.

Data Availability Statement: Data are contained within the article and Supplementary Materials.

Conflicts of Interest: The authors declare no conflict of interest.

References

1. Gregg, J.M.; Bish, D.L.; Kaczmarek, S.E.; Machel, H.G. Mineralogy, Nucleation and Growth of Dolomite in the Laboratory and Sedimentary Environment: A Review. *Sedimentology* **2015**, *62*, 1749–1769. [CrossRef]
2. Budd, D.A. Cenozoic Dolomites of Carbonate Islands: Their Attributes and Origin. *Earth Sci. Rev.* **1997**, *42*, 1–47. [CrossRef]
3. Blake, D.F.; Peacor, D.R.; Wilkinson, B.H. The Sequence and Mechanism of Low-Temperature Dolomite Formation; Calcian Dolomites in a Pennsylvanian Echinoderm. *J. Sediment. Res.* **1982**, *52*, 59–70. [CrossRef]
4. Goldsmith, J.R.; Graf, D.L. Structural and Compositional Variations in Some Natural Dolomites. *J. Geol.* **1958**, *66*, 678–693. [CrossRef]
5. Warren, J. Dolomite: Occurrence, Evolution and Economically Important Associations. *Earth Sci. Rev.* **2000**, *52*, 1–81. [CrossRef]
6. Holland, H.D.; Zimmermann, H. The Dolomite Problem Revisited1. *Int. Geol. Rev.* **2000**, *42*, 481–490. [CrossRef]
7. Machel, H.G. Concepts and Models of Dolomitization: A Critical Reappraisal. *Geol. Soc. Lond. Spec. Publ.* **2004**, *235*, 7–63. [CrossRef]
8. McKenzie, J.A.; Vasconcelos, C. Dolomite Mountains and the Origin of the Dolomite Rock of Which They Mainly Consist: Historical Developments and New Perspectives. *Sedimentology* **2009**, *56*, 205–219. [CrossRef]
9. Petrash, D.A.; Bialik, O.M.; Bontognali, T.R.R.; Vasconcelos, C.; Roberts, J.A.; McKenzie, J.A.; Konhauser, K.O. Microbially Catalyzed Dolomite Formation: From near-Surface to Burial. *Earth Sci. Rev.* **2017**, *171*, 558–582. [CrossRef]
10. Eriksson, P.G.; Banerjee, S.; Octavian, C.; Corcoran, P.; Eriksson, K.; Hiatt, E.; Laflamme, M.; Lenhardt, N.; Long, D.; Miall, A.; et al. Secular Changes in Sedimentation Systems and Sequence Stratigraphy. *Gondwana Res.* **2012**, *24*, 468–489. [CrossRef]
11. Pina, C.M.; Pimentel, C.; Crespo, Á. Dolomite Cation Order in the Geological Record. *Chem Geol* **2020**, *547*, 119667. [CrossRef]
12. Given, R.K.; Wilkinson, B.H. Dolomite Abundance and Stratigraphic Age; Constraints on Rates and Mechanisms of Phanerozoic Dolostone Formation. *J. Sediment. Res.* **1987**, *57*, 1068–1078. [CrossRef]
13. Balci, N.; Demirel, C.; Akcer Ön, S.; Gültekin, A.H.; Kurt, M.A. Evaluating Abiotic and Microbial Factors on Carbonate Precipitation in Lake Acigöl, a Hypersaline Lake in Southwestern Turkey. *Quat. Int.* **2018**, *486*, 116–128. [CrossRef]
14. Last, F.M.; Last, W.M.; Halden, N.M. Carbonate Microbialites and Hardgrounds from Manito Lake, an Alkaline, Hypersaline Lake in the Northern Great Plains of Canada. *Sediment. Geol.* **2010**, *225*, 34–49. [CrossRef]
15. Last, F.M.; Last, W.M.; Halden, N.M. Modern and Late Holocene Dolomite Formation: Manito Lake, Saskatchewan, Canada. *Sediment. Geol.* **2012**, *281*, 222–237. [CrossRef]
16. Vasconcelos, C.; McKenzie, J.A. Microbial Mediation of Modern Dolomite Precipitation and Diagenesis under Anoxic Conditions (Lagoa Vermelha, Rio de Janeiro, Brazil). *J. Sediment. Res.* **1997**, *67*, 378–390. [CrossRef]
17. Diloreto, Z.A.; Garg, S.; Bontognali, T.R.R.; Dittrich, M. Modern Dolomite Formation Caused by Seasonal Cycling of Oxygenic Phototrophs and Anoxygenic Phototrophs in a Hypersaline Sabkha. *Sci. Rep.* **2021**, *11*, 4170. [CrossRef] [PubMed]

18. Areias, C.; Barbosa, C.F.; Cruz, A.P.S.; McKenzie, J.A.; Ariztegui, D.; Eglinton, T.; Haghipour, N.; Vasconcelos, C.; Sánchez-Román, M. Organic Matter Diagenesis and Precipitation of Mg-Rich Carbonate and Dolomite in Modern Hypersaline Lagoons Linked to Climate Changes. *Geochim. Cosmochim. Acta* **2022**, *337*, 14–32. [CrossRef]
19. Perri, E.; Tucker, M.E.; Słowakiewicz, M.; Whitaker, F.; Bowen, L.; Perrotta, I.D. Carbonate and Silicate Biomineralization in a Hypersaline Microbial Mat (Mesaieed Sabkha, Qatar): Roles of Bacteria, Extracellular Polymeric Substances and Viruses. *Sedimentology* **2018**, *65*, 1213–1245. [CrossRef]
20. Samylina, O.S.; Zaytseva, L. V Characterization of Modern Dolomite Stromatolites from Hypersaline Petukhovskoe Soda Lake, Russia. *Lethaia* **2019**, *52*, 1–13. [CrossRef]
21. Bontognali, T.; Vasconcelos, C.; Warthmann, R.; Bernasconi, S.; Dupraz, C.; Strohmenger, C.; McKenzie, J. Dolomite Formation within Microbial Mats in the Coastal Sabkha of Abu Dhabi (United Arab Emirates). *Sedimentology* **2010**, *57*, 824–844. [CrossRef]
22. Mauger, C.; Compton, J. Formation of Modern Dolomite in Hypersaline Pans of the Western Cape, South Africa. *Sedimentology* **2011**, *58*, 1678–1692. [CrossRef]
23. Rosen, M.R.; Coshell, L. A New Location of Holocene Dolomite Formation, Lake Hayward, Western Australia. *Sedimentology* **1992**, *39*, 161–166. [CrossRef]
24. De Deckker, P.; Last, W.M. Modern Dolomite Deposition in Continental, Saline Lakes, Western Victoria, Australia. *Geology* **1988**, *16*, 29–32. [CrossRef]
25. Angeletti, L.; Canese, S.; Franchi, F.; Montagna, P.; Reitner, J.; Walliser, E.O.; Taviani, M. The "Chimney Forest" of the Deep Montenegrin Margin, South-Eastern Adriatic Sea. *Mar. Pet. Geol.* **2015**, *66*, 542–554. [CrossRef]
26. Bian, Y.; Feng, D.; Roberts, H.H.; Chen, D. Tracing the Evolution of Seep Fluids from Authigenic Carbonates: Green Canyon, Northern Gulf of Mexico. *Mar. Pet. Geol.* **2013**, *44*, 71–81. [CrossRef]
27. Li, J.; Peng, X.; Bai, S.; Chen, Z.; Van Nostrand, J.D. Biogeochemical Processes Controlling Authigenic Carbonate Formation within the Sediment Column from the Okinawa Trough. *Geochim. Cosmochim. Acta* **2018**, *222*, 363–382. [CrossRef]
28. Lu, Y.; Sun, X.; Lin, Z.; Xu, L.; Gong, J.; Lu, H. Cold Seep Status Archived in Authigenic Carbonates: Mineralogical and Isotopic Evidence from Northern South China Sea. *Deep. Sea Res. Part II Top. Stud. Oceanogr.* **2015**, *122*, 95–105. [CrossRef]
29. Magalhães, V.H.; Pinheiro, L.M.; Ivanov, M.K.; Kozlova, E.; Blinova, V.; Kolganova, J.; Vasconcelos, C.; McKenzie, J.A.; Bernasconi, S.M.; Kopf, A.J.; et al. Formation Processes of Methane-Derived Authigenic Carbonates from the Gulf of Cadiz. *Sediment. Geol.* **2012**, *243–244*, 155–168. [CrossRef]
30. Naehr, T.H.; Eichhubl, P.; Orphan, V.J.; Hovland, M.; Paull, C.K.; Ussler, W.; Lorenson, T.D.; Greene, H.G. Authigenic Carbonate Formation at Hydrocarbon Seeps in Continental Margin Sediments: A Comparative Study. *Deep. Sea Res. Part II Top. Stud. Oceanogr.* **2007**, *54*, 1268–1291. [CrossRef]
31. Stakes, D.S.; Orange, D.; Paduan, J.B.; Salamy, K.A.; Maher, N. Cold-Seeps and Authigenic Carbonate Formation in Monterey Bay, California. *Mar. Geol.* **1999**, *159*, 93–109. [CrossRef]
32. Takeuchi, R.; Matsumoto, R.; Ogihara, S.; Machiyama, H. Methane-Induced Dolomite "Chimneys" on the Kuroshima Knoll, Ryukyu Islands, Japan. *J. Geochem. Explor.* **2007**, *95*, 16–28. [CrossRef]
33. Cavagna, S.; Clari, P.; Martire, L. The Role of Bacteria in the Formation of Cold Seep Carbonates: Geological Evidence from Monferrato (Tertiary, NW Italy). *Sediment. Geol.* **1999**, *126*, 253–270. [CrossRef]
34. Wang, S.; Yan, W.; Chen, Z.; Zhang, N.; Chen, H. Rare Earth Elements in Cold Seep Carbonates from the Southwestern Dongsha Area, Northern South China Sea. *Mar. Pet. Geol.* **2014**, *57*, 482–493. [CrossRef]
35. Sun, W.; Jayaraman, S.; Chen, W.; Persson, K.A.; Ceder, G. Nucleation of Metastable Aragonite CaCO3 in Seawater. *Proc. Natl. Acad. Sci. USA* **2015**, *112*, 3199–3204. [CrossRef] [PubMed]
36. Sandberg, P.A. An Oscillating Trend in Phanerozoic Non-Skeletal Carbonate Mineralogy. *Nature* **1983**, *305*, 19–22. [CrossRef]
37. Hardie, L.A. Secular Variation in Seawater Chemistry: An Explanation for the Coupled Secular Variation in the Mineralogies of Marine Limestones and Potash Evaporites over the Past 600 m.y. *Geology* **1996**, *24*, 279–283. [CrossRef]
38. Stanley, S.M.; Hardie, L.A. Secular Oscillations in the Carbonate Mineralogy of Reef-Building and Sediment-Producing Organisms Driven by Tectonically Forced Shifts in Seawater Chemistry. *Palaeogeogr. Palaeoclimatol. Palaeoecol.* **1998**, *144*, 3–19. [CrossRef]
39. Morse, J.W.; Wang, Q.; Tsio, M.Y. Influences of Temperature and Mg:Ca Ratio on $CaCO_3$ Precipitates from Seawater. *Geology* **1997**, *25*, 85–87. [CrossRef]
40. Hood, A.v.S.; Wallace, M.W.; Drysdale, R.N. Neoproterozoic Aragonite-Dolomite Seas? Widespread Marine Dolomite Precipitation in Cryogenian Reef Complexes. *Geology* **2011**, *39*, 871–874. [CrossRef]
41. Van Smeerdijk Hood, A.; Wallace, M.W. Synsedimentary Diagenesis in a Cryogenian Reef Complex: Ubiquitous Marine Dolomite Precipitation. *Sediment. Geol.* **2012**, *255–256*, 56–71. [CrossRef]
42. Lu, Y.; Paulmann, C.; Mihailova, B.; Malcherek, T.; Birgel, D.; López Correa, M.; Lin, Z.; Lu, L.; Milker, Y.; Peckmann, J. Fibrous Dolomite Formation at a Miocene Methane Seep May Reflect Neoproterozoic Aragonite-Dolomite Sea Conditions. *Commun. Earth Environ.* **2023**, *4*, 346. [CrossRef]
43. Zhang, F.; Xu, H.; Konishi, H.; Kemp, J.M.; Roden, E.E.; Shen, Z. Dissolved Sulfide-Catalyzed Precipitation of Disordered Dolomite: Implications for the Formation Mechanism of Sedimentary Dolomite. *Geochim. Cosmochim. Acta* **2012**, *97*, 148–165. [CrossRef]
44. Lippmann, F. The Polymorphism Calcite-Aragonite. In *Sedimentary Carbonate Minerals*; Lippmann, F., Ed.; Springer: Berlin/Heidelberg, Germany, 1973; pp. 97–147. ISBN 978-3-642-65474-9.

45. Katz, A.K.; Glusker, J.P.; Markham, G.D.; Bock, C.W. Deprotonation of Water in the Presence of Carboxylate and Magnesium Ions. *J. Phys. Chem. B* **1998**, *102*, 6342–6350. [CrossRef]
46. Xu, J.; Yan, C.; Zhang, F.; Konishi, H.; Xu, H.; Teng, H. Testing the Cation-Hydration Effect on the Crystallization of Ca-Mg-CO_3 Systems. *Proc. Natl. Acad. Sci. USA* **2013**, *110*, 17750–17755. [CrossRef] [PubMed]
47. Lindner, M.; Saldi, G.D.; Jordan, G.; Schott, J. On the Effect of Aqueous Barium on Magnesite Growth—A New Route for the Precipitation of the Ordered Anhydrous Mg-Bearing Double Carbonate Norsethite. *Chem. Geol.* **2017**, *460*, 93–105. [CrossRef]
48. Pimentel, C.; Pina, C.M. The Formation of the Dolomite-Analogue Norsethite: Reaction Pathway and Cation Ordering. *Geochim. Cosmochim. Acta* **2014**, *142*, 217–223. [CrossRef]
49. Zhang, Y.-F.; Yao, Q.-Z.; Qian, F.-J.; Li, H.; Zhou, G.-T.; Fu, S.-Q. Formation Pathway of Norsethite Dominated by Solution Chemistry under Ambient Conditions. *Am. Mineral.* **2021**, *106*, 1306–1318. [CrossRef]
50. Zhang, F.; Xu, H.; Konishi, H.; Shelobolina, E.S.; Roden, E.E. Polysaccharide-Catalyzed Nucleation and Growth of Disordered Dolomite: A Potential Precursor of Sedimentary Dolomite. *Am. Mineral.* **2012**, *97*, 556–567. [CrossRef]
51. Roberts, J.; Kenward, P.; Fowle, D.; Goldstein, R.; Gonzalez, L.; Moore, D. Surface Chemistry Allows for Abiotic Precipitation of Dolomite at Low Temperature. *Proc. Natl. Acad. Sci. USA* **2013**, *110*, 14540–14545. [CrossRef]
52. Zhang, F.; Xu, H.; Shelobolina, E.S.; Konishi, H.; Converse, B.; Shen, Z.; Roden, E.E. The Catalytic Effect of Bound Extracellular Polymeric Substances Excreted by Anaerobic Microorganisms on Ca-Mg Carbonate Precipitation: Implications for the "Dolomite Problem". *Am. Mineral.* **2015**, *100*, 483–494. [CrossRef]
53. Shen, Z.; Szlufarska, I.; Brown, P.E.; Xu, H. Investigation of the Role of Polysaccharide in the Dolomite Growth at Low Temperature by Using Atomistic Simulations. *Langmuir* **2015**, *31*, 10435–10442. [CrossRef] [PubMed]
54. Vasconcelos, C.; McKenzie, J.A.; Bernasconi, S.; Grujic, D.; Tiens, A.J. Microbial Mediation as a Possible Mechanism for Natural Dolomite Formation at Low Temperatures. *Nature* **1995**, *377*, 220–222. [CrossRef]
55. Wright, D.T. The Role of Sulphate-Reducing Bacteria and Cyanobacteria in Dolomite Formation in Distal Ephemeral Lakes of the Coorong Region, South Australia. *Sediment. Geol.* **1999**, *126*, 147–157. [CrossRef]
56. Warthmann, R.; van Lith, Y.; Vasconcelos, C.; McKenzie, J.A.; Karpoff, A.M. Bacterially Induced Dolomite Precipitation in Anoxic Culture Experiments. *Geology* **2000**, *28*, 1091–1094. [CrossRef]
57. Van Lith, Y.; Warthmann, R.; Vasconcelos, C.; Mckenzie, J.A. Sulphate-Reducing Bacteria Induce Low-Temperature Ca-Dolomite and High Mg-Calcite Formation. *Geobiology* **2003**, *1*, 71–79. [CrossRef]
58. Roberts, J.A.; Bennett, P.C.; González, L.A.; Macpherson, G.L.; Milliken, K.L. Microbial Precipitation of Dolomite in Methanogenic Groundwater. *Geology* **2004**, *32*, 277–280. [CrossRef]
59. Wright, D.T.; Wacey, D. Precipitation of Dolomite Using Sulphate-Reducing Bacteria from the Coorong Region, South Australia: Significance and Implications. *Sedimentology* **2005**, *52*, 987–1008. [CrossRef]
60. Sánchez-Román, M.; Vasconcelos, C.; Schmid, T.; Dittrich, M.; McKenzie, J.A.; Zenobi, R.; Rivadeneyra, M.A. Aerobic Microbial Dolomite at the Nanometer Scale: Implications for the Geologic Record. *Geology* **2008**, *36*, 879–882. [CrossRef]
61. Kenward, P.A.; Goldstein, R.H.; González, L.A.; Roberts, J.A. Precipitation of Low-Temperature Dolomite from an Anaerobic Microbial Consortium: The Role of Methanogenic Archaea. *Geobiology* **2009**, *7*, 556–565. [CrossRef]
62. Bontognali, T.; Vasconcelos, C.; Warthmann, R.; Lundberg, R.; McKenzie, J. Dolomite-mediating Bacterium Isolated from the Sabkha of Abu Dhabi (UAE). *Terra Nova* **2012**, *24*, 248–254. [CrossRef]
63. Alibrahim, A.; Al-Gharabally, D.; Mahmoud, H.; Dittrich, M. Proto-Dolomite Formation in Microbial Consortia Dominated by Halomonas Strains. *Extremophiles* **2019**, *23*, 765–781. [CrossRef] [PubMed]
64. Daye, M.; Higgins, J.; Bosak, T. Formation of Ordered Dolomite in Anaerobic Photosynthetic Biofilms. *Geology* **2019**, *47*, 509–512. [CrossRef]
65. Deng, S.; Dong, H.; Lv, G.; Jiang, H.; Yu, B.; Bishop, M.E. Microbial Dolomite Precipitation Using Sulfate Reducing and Halophilic Bacteria: Results from Qinghai Lake, Tibetan Plateau, NW China. *Chem. Geol.* **2010**, *278*, 151–159. [CrossRef]
66. Qiu, X.; Yao, Y.; Wang, H.; Shen, A.; Zhang, J. Halophilic Archaea Mediate the Formation of Proto-Dolomite in Solutions With Various Sulfate Concentrations and Salinities. *Front. Microbiol.* **2019**, *10*, 480. [CrossRef] [PubMed]
67. Sánchez-Román, M.; Vasconcelos, C.; Warthmann, R.; Rivadeneyra, M.; McKenzie, J.A. Microbial Dolomite Precipitation under Aerobic Conditions: Results from Brejo Do Espinho Lagoon (Brazil) and Culture Experiments. In *Perspectives in Carbonate Geology: A Tribute to the Career of Robert Nathan Ginsburg*; International Association of Sedimentologists: Gent, Belgium, 2009; pp. 167–178.
68. Zheng, T.; Qian, C. Influencing Factors and Formation Mechanism of $CaCO_3$ Precipitation Induced by Microbial Carbonic Anhydrase. *Process Biochem.* **2020**, *91*, 271–281. [CrossRef]
69. Zhang, F.; Xu, H.; Shelobolina, E.S.; Konishi, H.; Roden, E.E. Precipitation of Low-Temperature Disordered Dolomite Induced by Extracellular Polymeric Substances of Methanogenic Archaea Methanosarcina Barkeri: Implications for Sedimentary Dolomite Formation. *Am. Mineral.* **2021**, *106*, 69–81. [CrossRef]
70. Fan, Q.; Liu, D.; Papineau, D.; Qiu, X.; Wang, H.; She, Z.; Zhao, L. Precipitation of High Mg-Calcite and Protodolomite Using Dead Biomass of Aerobic Halophilic Bacteria. *J. Earth Sci.* **2023**, *34*, 456–466. [CrossRef]
71. Bontognali, T.R.R.; McKenzie, J.A.; Warthmann, R.J.; Vasconcelos, C. Microbially Influenced Formation of Mg-Calcite and Ca-Dolomite in the Presence of Exopolymeric Substances Produced by Sulphate-Reducing Bacteria. *Terra Nova* **2014**, *26*, 72–77. [CrossRef]

72. Kim, J.; Kimura, Y.; Puchala, B.; Yamazaki, T.; Becker, U.; Sun, W. Dissolution Enables Dolomite Crystal Growth near Ambient Conditions. *Science (1979)* **2023**, *382*, 915–920. [CrossRef]
73. Hasegawa, M.; Konishi, H.; Kubota, Y. Inorganic Synthesis of Disordered Dolomite at Room Temperature. In Proceedings of the Goldschmidt, Lyon, France, 9–14 July 2023.
74. Royse, C.F.; Wadell, J.S.; Petersen, L.E. X-Ray Determination of Calcite-Dolomite: An Evaluation. *J. Sediment. Res.* **1971**, *41*, 483–488. [CrossRef]
75. Lumsden, D.N.; Chimahusky, J.S. Relationship between Dolomite Nonstoichiometry and Carbonate Facies Parameters. In *Concepts and Models of Dolomitization*; Zenger, D.H., Dunham, J.B., Ethington, R.L., Eds.; Special Publication; Society of Economic Paleontologists and Mineralogists: Claremore, OK, USA, 1980; Volume 28, pp. 123–137.
76. Füchtbauer, H.; Goldschmidt, H. Beziehungen Zwischen Calciumgehalt Und Bildungsbedingungen Der Dolomite. *Geol. Rundsch.* **1966**, *55*, 29–40. [CrossRef]
77. Sibley, D.F.; Nordeng, S.H.; Borkowski, M.L. Dolomitization Kinetics of Hydrothermal Bombs and Natural Settings. *J. Sediment. Res.* **1994**, *64*, 630–637. [CrossRef]
78. Kaczmarek, S.E.; Sibley, D.F. On the Evolution of Dolomite Stoichiometry and Cation Order during High-Temperature Synthesis Experiments: An Alternative Model for the Geochemical Evolution of Natural Dolomites. *Sediment. Geol.* **2011**, *240*, 30–40. [CrossRef]
79. Kaczmarek, S.E.; Sibley, D.F. Direct Physical Evidence of Dolomite Recrystallization. *Sedimentology* **2014**, *61*, 1862–1882. [CrossRef]
80. Li, J.; Chen, F.; Song, N.; Li, B.; Ma, Y. Investigation on the Influence of Additives on the Oriented Dissolution of Calcite. *Soft Matter* **2021**, *17*, 5025–5033. [CrossRef] [PubMed]
81. Zhang, Y.; Li, J.; Qi, L.; Ma, Y. Investigation of the Influence of Cationic and Anionic Ions on the Oriented Dissolution of Calcite. *CrystEngComm* **2020**, *22*, 5316–5322. [CrossRef]
82. Meng, R.; Ma, Y.; Long, X.; Qi, L. Calcite Microrod Arrays Fabricated via Anisotropic Dissolution of Calcite in the Presence of NH_4I and $(NH_4)_2SO_4$. *CrystEngComm* **2013**, *15*, 8867–8873. [CrossRef]
83. Long, X.; Meng, R.; Wu, W.; Ma, Y.; Qi, L. Calcite Microneedle Arrays Produced by Inorganic Ion-Assisted Anisotropic Dissolution of Bulk Calcite Crystal. *Chemistry* **2014**, *20*, 4264–4272. [CrossRef]
84. Gutjahr, A.; Dabringhaus, H.; Lacmann, R. Studies of the Growth and Dissolution Kinetics of the $CaCO_3$ Polymorphs Calcite and Aragonite II. The Influence of Divalent Cation Additives on the Growth and Dissolution Rates. *J. Cryst. Growth* **1996**, *158*, 310–315. [CrossRef]
85. Parsiegla, K.I.; Katz, J.L. Calcite Growth Inhibition by Copper(II): II. Effect of Solution Composition. *J. Cryst. Growth* **2000**, *213*, 368–380. [CrossRef]
86. Vinson, M.D.; Arvidson, R.S.; Luttge, A. Kinetic Inhibition of Calcite (104) Dissolution by Aqueous Manganese(II). *J. Cryst. Growth* **2007**, *307*, 116–125. [CrossRef]
87. Olsen, R.; Leirvik, K.N.; Kvamme, B. Adsorption Characteristics of Glycols on Calcite and Hematite. *AIChE J.* **2019**, *65*, e16728. [CrossRef]
88. Tang, H.; Xian, H.; He, H.; Wei, J.; Liu, H.; Zhu, J.; Zhu, R. Kinetics and Mechanisms of the Interaction between the Calcite (10.4) Surface and Cu^{2+}-Bearing Solutions. *Sci. Total Environ.* **2019**, *668*, 602–616. [CrossRef] [PubMed]
89. Dong, S.; Berelson, W.M.; Adkins, J.F.; Rollins, N.E.; Naviaux, J.D.; Pirbadian, S.; El-Naggar, M.Y.; Teng, H.H. An Atomic Force Microscopy Study of Calcite Dissolution in Seawater. *Geochim. Cosmochim. Acta* **2020**, *283*, 40–53. [CrossRef]
90. Gagić, T.; Perva-Uzunalić, A.; Knez, Ž.; Škerget, M. Hydrothermal Degradation of Cellulose at Temperature from 200 to 300 °C. *Ind. Eng. Chem. Res.* **2018**, *57*, 6576–6584. [CrossRef]
91. Machel, H. Investigation of Burial Diagenesis in Carbonate Hydrocarbon Reservoir Rocks. *Geosci. Can.* **2005**, *32*, 103–128.
92. Veetil, S.P.; Mucci, A.; Arakaki, T. Dolomite Dissolution Kinetics in Aqueous Solutions in the Presence of Organic and Inorganic Additives at 25 °C and PCO2~1 atm. *Chem. Geol.* **2018**, *483*, 98–110. [CrossRef]

Disclaimer/Publisher's Note: The statements, opinions and data contained in all publications are solely those of the individual author(s) and contributor(s) and not of MDPI and/or the editor(s). MDPI and/or the editor(s) disclaim responsibility for any injury to people or property resulting from any ideas, methods, instructions or products referred to in the content.